Korean J. Chem. Eng., **30**(8), 1594-1602 (2013)
DOI: 10.1007/s11814-013-0079-7

Synthesis of a new low-cost activated carbon from activated sludge for the removal of Cr (VI) from aqueous solution: Equilibrium, kinetics, thermodynamics and desorption studies

Fatemeh Gorzin and Ali Asghar Ghoreyshi†

Department of Chemical Engineering, Babol University of Technology, Babol, Iran
(*Received 23 February 2013 • accepted 6 May 2013*)

Abstract−Elimination of Cr (VI) from aqueous solution was investigated by a new low cost activated carbon developed from aerobically digested activated sludge (ADAS). The adsorbent demonstrated remarkable characteristics such as high surface area of 760 $m^2 \cdot g^{-1}$ and large total pore volume of 0.8383 $cm^3 \cdot g^{-1}$. The maximum equilibrium uptake of Cr (VI) was 70.15 $mg \cdot g^{-1}$ at optimum pH 2.0. Interpretation of equilibrium data revealed that the best description was provided by the Freundlich isotherm. The kinetics of Cr (VI) adsorption was well described by the pseudo-second order equation. Calculation of thermodynamic parameters revealed that the adsorption process was endothermic, spontaneous and feasible. The adsorbent was regenerated using NaOH and it was found to be suitable for reuse in successive adsorption-desorption cycles. The desorption efficiency of Cr (VI) ion was up to 78%. Finally, comparison of Cr (VI) adsorption capacity of the developed adsorbent with commercial activated carbon demonstrated its higher performance.

Key words: Cr (VI), Adsorption Isotherm, Activated Carbon, Kinetics, Thermodynamics, Activated Sludge

INTRODUCTION

Chromium compounds are commonly released into the environment by the effluents of industrial plants such as electroplating, leather tanning, textile dyeing and wood preservations [1]. Chromium exists in two stable and common oxidation states: hexavalent and trivalent forms. Due to its high water solubility, Cr (VI) is very toxic, carcinogenic and mutagenic to animals and human health compared to trivalent chromium form [2]. According to United States Environmental Protection Agency (USEPA), the maximum allowable Cr (VI) level in drinking water is 0.05 $mg \cdot l^{-1}$ and for discharge into inland surface waters is 0.1 $mg \cdot l^{-1}$; hence, it is essential to be removed from wastewater before its discharge into the environment [3,4]. A wide range of treatment methods for the removal of Cr (VI) from industrial wastewaters have been employed including ion exchange [5], electrochemical reduction [6], solvent extraction [7], chemical coagulation [8], agricultural waste [9], reverse osmosis [10], and adsorption [11]. Most of these methods have disadvantages such as high capital and operational costs, incomplete metal removal, generation of toxic sludge and high chemicals and energy requirements [12]. Among these methods, adsorption onto solid materials is considered as an effective, efficient, and economic method and has been frequently used to eliminate toxic pollutants from industrial wastewaters [13]. Activated carbon is widely used for the removal of hexavalent chromium from wastewater due to its high surface area, chemical stability and active functional groups. However, the high cost associated with commercial coal-based activated carbon limits its utilization in wastewater treatment [14]. In recent years, removal of hexavalent chromium from wastewater has been reported to be cheap and efficient using activated carbons prepared from lignocelluloses materials such as rice husk [15], coconut shell [16], fertilizer industry waste material [3], Ocimum americanum seed pods [12], Eichhornia crassipes root [17], peanut shell [18], hazelnut shell [19], olive oil industry waste [20], sawdust [21], distillery sludge [22], etc. Typical capacities of Cr (VI) adsorption by these adsorbents are presented in Table 1.

The disposal of sludge is a major problem worldwide due to the tremendous amount of wastewater treatment activities. Conventional disposal methods such as land filling, incineration and conversion to fertilizer have been used to remove municipal and industrial sludge from environment. However these methods are relatively expensive and have important limitations such as soil and air pollutions. Using sewage sludge as a carbonaceous raw material offers the dual benefits of reduction in the sludge volume and production of an effective adsorbent with lower cost than commercial activated carbons [23].

Our goal was to develop new, low-cost activated carbon as an effective adsorbent for the removal of Cr (VI) from water. The new adsorbent was synthesized from aerobically digested activated sludge (ADAS) by chemical activation with $ZnCl_2$ followed by high temperature carbonization in an inert atmosphere. The influence of different parameters such as adsorbent dosage, pH, contact time, initial ion concentration, and temperature on hexavalent chromium adsorption was investigated. BET, SEM-EDX and FTIR analyses were performed to determine different physiochemical characteristics of the developed activated carbon. The equilibria, kinetics and thermodynamics of adsorption were theoretically interpreted by means of different models. The activated carbon was effectively regenerated by conducting desorption experiments with different concentrations of NaOH.

MATERIALS AND METHODS

The ADAS for the synthesis of activated carbon was collected

†To whom correspondence should be addressed.
E-mail: aa_ghoreyshi@nit.ac.ir

Table 1. Comparison of Cr (VI) adsorption capacities of activated carbon prepared from different low cost materials

Adsorbent	Maximum Cr (VI) concentration ($mg \cdot l^{-1}$)	pH	Adsorption capacity ($mg \cdot g^{-1}$)	Reference
Fertilizer industry waste	100	2	15.24	[3]
Sawdust	200	2	65.8	[21]
Rice husk	200	2	52.1	[15]
Coconut shell charcoal	25	4	10.88	[16]
Peanut shell	100	2	8.31	[18]
Ocimum americanum seed pods	200	1.5	83.33	[12]
E. crassipes root biomass	100	4.5	36.34	[17]
Hazelnut shell	1000	1	170	[19]
Olive oil industry waste	200	2	18.69	[20]
Distillery sludge	25	3	5.7	[22]
The ADAS-based activated carbon	250	2	70.15	This study

Table 2. Proximate and ultimate analyses of the ADAS (results are expressed on a dry basis, except for the humidity)

	Ultimate analysis (wt%)			Proximate analysis	
Parameter	C	H	N	Humidity (%)	Ash
Value	36.05	6.22	8.21	14.71	11.28

from the wastewater treatment plant of a local dairy industry, Amol, Iran. The commercial activated carbon (code: 1.02183.100) was produced from charcoal provided by Merck Co., Germany. All reagents used in this study were analytical grade and also supplied by Merck Co., Germany, and were used without further purification. A stock solution of 1,000 $mg \cdot l^{-1}$ Cr (VI) ions was prepared by dissolving 2.8289 g of potassium dichromate in distilled water. The required lower concentrations were prepared by dilution of the stock solution with distilled water when necessary.

1. Synthesis and Characterization of Activated Carbon

Proximate and ultimate analyses of the ADAS are given in Table 2. Raw materials were first dried at 110 °C for 24 h in an oven, then crushed and sieved into particles with diameters of less than 0.6 mm. To activate the crushed materials, they were soaked in 5 M $ZnCl_2$ solution with an impregnation ratio of 3 : 1 ($ZnCl_2$: dry sludge wt%) and well mixed at 85 °C for 8 h using magnetic stirrer. After chemical activation, samples were dried at 110 °C for 24 h in an oven. Carbonization of the chemically activated ADAS was carried out in an inert atmosphere in a horizontal furnace at 650 °C for 1 h under the nitrogen flow of 400 $ml \cdot min^{-1}$, while the heating rate was kept at 10 $°C \cdot min^{-1}$. The resulting samples were washed with 1 M HCl and then with distilled water until pH reached to lower than 6 to remove excess zinc chloride and residual inorganic matter. Finally, the rinsed products were dried at 110 °C in an oven.

The textural properties of the activated carbon prepared from ADAS including BET surface area, pore size distribution and total pore volume were determined by using N_2 adsorption/desorption isotherm at 77 K in a surface area analyzer (BELsorp-mini II, Japan). The surface area was calculated by the Brunauer-Emmet-Teller (BET) equation. The pore size distribution of the adsorbent was determined by the Barrett-Joyner-Halenda (BJH) method. Micropore volume was obtained according the t-plot method. Mesopore volume was calculated by the difference between the total pore volume (p/p_0= 0.99) and micropore volume [24]. The morphology of the developed adsorbent was studied by scanning electron microscopy (SEM, VEGA II TESCAN, CZECH). The qualitative elemental composition of the adsorbent was analyzed using energy dispersive X-ray spectroscopy (EDX), (VEGA II TESCAN, CZECH). Fourier transform infrared spectra (FTIR) of the adsorbent before and after adsorption of Cr (VI) was obtained in the frequency range of 400-4,000 cm^{-1} using Shimadzu, FTIR1650 spectrophotometer, Japan.

2. Adsorption Experiments

Adsorption experiments were carried out in an incubator shaker (model KS 4000i control, IKA) rotating at 180 rpm. For each experimental run, a 0.15 g of adsorbent per 50 ml of the chromium solution (3 $g \cdot l^{-1}$) was used in a 250 ml Erlenmeyer flask. The influences of main affecting parameters on the amount of adsorption in the specified ranges, i.e., pH (2-8); initial chromium concentration (50-250 $mg \cdot l^{-1}$); contact time (0-120 min) and temperature (25-45 °C) were investigated. The solution pH was adjusted using either 0.1 N HCl or 0.1 N NaOH solutions. After shaking, samples were filtered through a Whatman No.42 filter paper. UV visible spectrophotometer (model 2100 SERIES, UNICO) was employed in acidic solution with 1, 5 diphenyl-carbazide at 540 nm to determine the concentrations of Cr (VI) in the sample [25].

The amount of metal ion adsorbed, q_t ($mg \cdot g^{-1}$) and removal efficiency (R %) achieved by the activated carbon were calculated according to Eqs. (1) and (2):

$$q_t = \frac{C_0 V_0 - C_t V_t}{m} \quad (1)$$

$$\%R = \frac{C_0 - C_e}{C_0} \times 100 \quad (2)$$

where q_t ($mg \cdot g^{-1}$) is the amount of Cr (VI) adsorbed per unit weight of activated carbon at time t, C_0 and C_e ($mg \cdot l^{-1}$) are the initial and final concentrations, C_t ($mg \cdot l^{-1}$) is the Cr (VI) concentration at time t, V_0 is the volume of the initial Cr (VI) solution (ml), V_t is the volume of the Cr (VI) solution at time t (ml) and m (g) is the weight of activated carbon.

3. Batch Desorption Study

To estimate the recovery of Cr (VI) ions from the adsorbent, desorption experiments can be conducted with different desorbing solutions: H_2SO_4, HCL, HNO_3 and NaOH. However, in this study

it makes sense to use NaOH as the desorption agent as the hydroxyl ions could increase the solution pH (potentially reversing the surface charge of the carbon and changing Cr (VI) speciation) and compete with the Cr (VI) anions. To optimize the required concentration of NaOH solution for maximum recovery of Cr (VI) ions from the adsorbent, desorption experiments were carried out in the concentration range of 0.1-0.5 N of NaOH solution. At first cycle, 10 ml of Cr (VI) solution with initial concentration of 50 $mg \cdot l^{-1}$, pH 2.0 and 3.5 $g \cdot l^{-1}$ of the adsorbent was shaken at 45 °C for 120 min in a 20 ml centrifuge tube. The solution was subsequently separated from the adsorbent by using centrifugation at 2,000 rpm for 20 min. The residual Cr (VI) content in the removed solution was measured to calculate the percentage of adsorption, while the adsorbent was kept in the tube at all stages. Then NaOH solution (0.5 N) was added to adsorbent and shaken at 45 °C for 120 min for desorption purpose. Finally, the solution was centrifuged (at 2,000 rpm for 20 min) and the residual concentration of Cr (VI) ions in the solution was measured to determine the percentage of desorption. Adsorbent was washed each time with distilled water until pH reached to neutral and was used for several cycles adsorption-desorption experiments. Sample was collected after 120 min to evaluate Cr (VI) recovery by the following equation:

$$\text{Metal recovery} = \frac{\text{Amount of metal ion desorbed}}{\text{Amount of metal ion adsorbed}} \times 100 \quad (3)$$

RESULTS AND DISCUSSION

1. Characterization Results

1-1. BET Surface Area

Fig. 1 shows the N_2 adsorption-desorption isotherms obtained for the developed activated carbon and commercial activated carbon at 77 K. BET surface area (S_{BET}) was determined by a surface area analyzer. It is clear from the Fig. 1 that the amount of nitrogen adsorbed by the ADAS-based activated carbon was higher than commercial one due to its high total pore volume and porosity. The adsorption curves show a gradual increase in N_2 adsorption volume after a sharp increase, which indicates a combination of microporous and mesoporous structure for the both adsorbents. The textural properties of the ADAS-based activated carbon and commercial activated carbon including surface area, porous volume and average pore diameter calculated from N_2 adsorption isotherms are given in Table 3. These values are much higher than previously reported mesoporous activated carbon produced by chemical activation with $ZnCl_2$ by Liu et al. [23]. They prepared activated carbons from sewage sludge with and without pyrolusite (mineral additive) and evaluated effect of pyrolusite content on mesoporosity and surface area of adsorbent. They have employed these adsorbents for removal of dye from wastewater. They have shown that adding pyrolusite caused an increase in mesoporosity in the range of 0.06-0.105 $cm^3 \cdot g^{-1}$ and BET surface area in the range of 88.9-210.2 $m^2 \cdot g^{-1}$. However, the ADAS-based activated carbon synthesized in this study possesses mesoporosity of 0.4116 $cm^3 \cdot g^{-1}$ and BET surface area of 760 $m^2 \cdot g^{-1}$, which represents higher characterization results compared to results obtained by Lie et al. in terms of BET analysis. This may be due to low percentage of ash in the ADAS precursor.

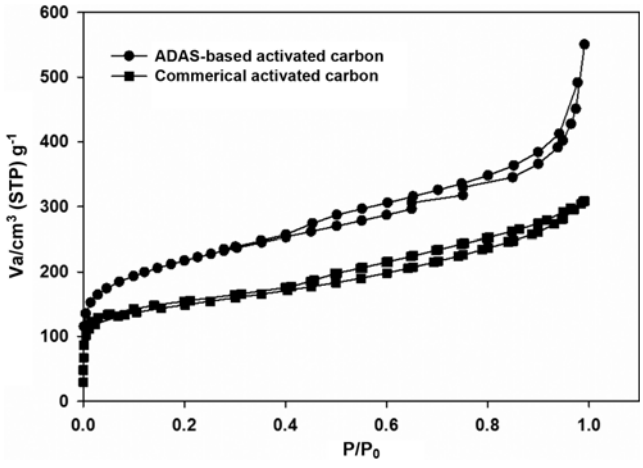

Fig. 1. Nitrogen adsorption-desorption isotherms for ADAS-based activated carbon and commercial activated carbon.

Table 3. Surface area and porosity of the ADAS-based activated carbon and commercial coal-based activated carbon

Properties	ADAS-based activated carbon	Commercial coal-based activated carbon
BET surface area ($m^2 \cdot g^{-1}$)	760	545.27
Total pore volume ($cm^3 \cdot g^{-1}$)	0.8383	0.4760
Micropore volume ($cm^3 \cdot g^{-1}$)	0.4267	0.2512
Mesoporosity (%)	49	47
Average pore diameter (nm)	3.9946	3.4916

According to IUPAC classification, this activated carbon with average pore diameter of 3.9946 nm ($2 \le d \le 50$) is classified into mesoporous material and represents the type (VI) isotherm [26]. High surface area and pore volume obtained for the developed adsorbent in this study is promising compared to the commercial one.

1-2. SEM-EDX Analysis

The surface morphology of the ADAS-based activated carbon before and after adsorption of Cr (VI) was evaluated by SEM-EDX spectrum as shown in Fig. 2(a) and (b). From Fig. 2(a), the prepared adsorbent had an irregular and porous surface containing different size and shapes, which accounts for its high surface area and pore volume. From Fig. 2(b) it is clear that the surface of the adsorbent shows to be smoother and also some small pores were closed due to surface coverage by the adsorbate. The new peak observed in the EDX spectrum in Fig. 2(b) compared to Fig. 2(a) can be attributed to the chromium adsorption onto the adsorbent surface. By comparing the EDX spectra of the activated carbon before and after chromium (VI) adsorption, the coverage of adsorbed Cr (VI) on the adsorbent surface is obvious after adsorption.

1-3. FTIR Spectroscopy Investigations

We used the FTIR spectra of the activated carbon before and after adsorption of Cr (VI) to identify functional groups on the adsorbent and the results are shown in Fig. 3(a) and (b). The changes in FTIR spectra may be due to the interaction of Cr (VI) ions with different functional groups such as carboxyl, hydroxyl and amino groups on the surface of the adsorbent [27]. The broad absorption band observed at 3,422.52 cm^{-1}, which was shifted to 3,432.42 cm^{-1} after adsorption, indicates complexation between -OH groups [28]. The

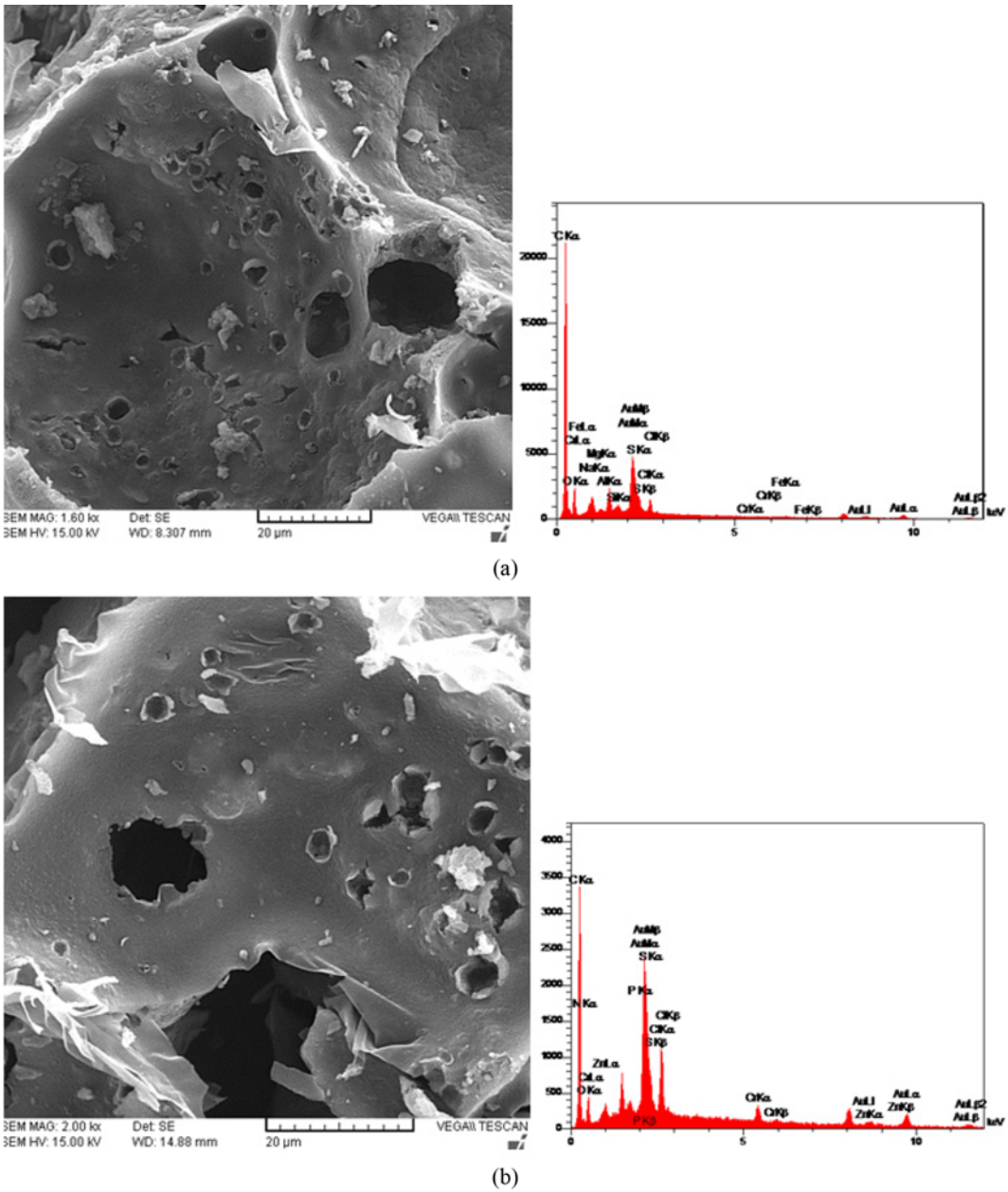

Fig. 2. SEM-EDX of synthesized activated carbon from ADAS (a) before and (b) after Cr (VI) adsorption.

absorption bands at 2,922 cm^{-1} could be attributed to C-H groups on the activated carbon. The peak at 1,618 cm^{-1} shifted to 1,612 cm^{-1} may represent complexation between hexavalent chromium with carboxylic group [29]. Another peak observed in the frequency range of 1,004 to 1,033 cm^{-1} may be due to interaction between nitrogen in amino groups with hexavalent chromium ions [9].

2. Adsorption Results

2-1. Effect of pH

The pH of the solution is one of the most important factors which affect the adsorption capacity of Cr (VI) ions by the adsorbent. The effect of pH on the removal efficiency of Cr (VI) by the synthesized activated carbon was studied in the pH range of 2.0-8.0, while adsorbent dosage, initial metal concentration and temperature were kept constant at 3 $g \cdot l^{-1}$, 50 $mg \cdot l^{-1}$ and 35 °C, respectively. Fig. 4 shows that the Cr (VI) removal efficiency dropped from 99.8% to 87.7% while pH increased from 2 to 3 and reached to 13.18% at the pH of 8. The results indicated that the maximum Cr (VI) removal percentage by the prepared activated carbon occurred at pH 2.0. Hence, the pH value of 2.0 was chosen as the optimal pH for further Cr (VI) adsorption experiments. The reasons for the higher Cr (VI) adsorption on a number of adsorbents at low pH values have been well addressed by many researchers [3,11,30]. At lower pH, the increase observed in Cr (VI) removal by the adsorbent is due to increase of H^+ ions on the adsorbent surface, which produces a strong electrostatic attraction between negatively charged hexavalent chromium ions ($Cr_2O_7^{2-}$, CrO_4^{2-}, etc.) and positively charged functional groups on the adsorbent surface [3]. Further decrease in Cr (VI) removal with increase in pH values from 2.0 to 8.0 may be due to increase in the concentration of hydroxyl ions on the adsorbent surface which develop a repulsive force between the oxy-anions and

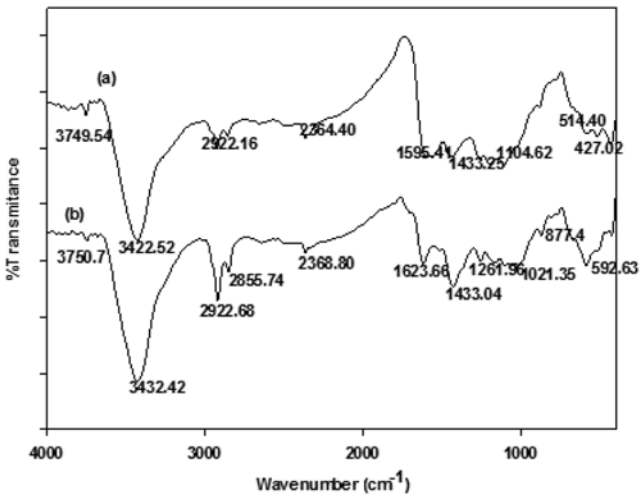

Fig. 3. FTIR spectra of the synthesized activated carbon from ADAS (a) pristine unloaded activated carbon and (b) activated carbon with loaded Cr (VI).

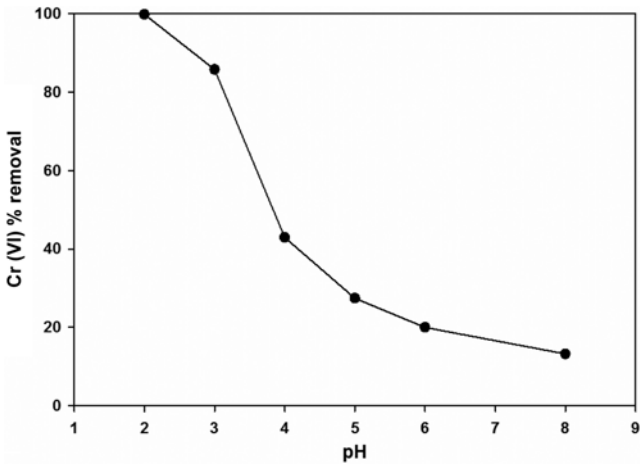

Fig. 4. Effect of initial pH on removal efficiency of Cr (VI) (C_0= 50 mg·l^{-1}, T=35 °C and adsorbent dose=3 g·l^{-1}).

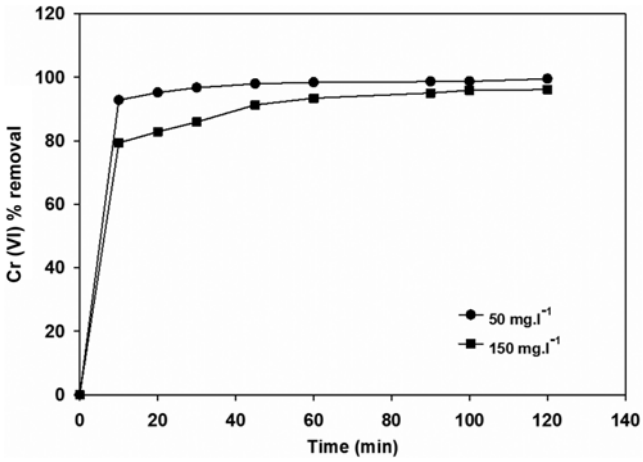

Fig. 5. Effect of contact time on removal efficiency of Cr (VI) (C_0= 50, 150 mg·l^{-1}, T=25 °C and adsorbent dose=3 g·l^{-1}).

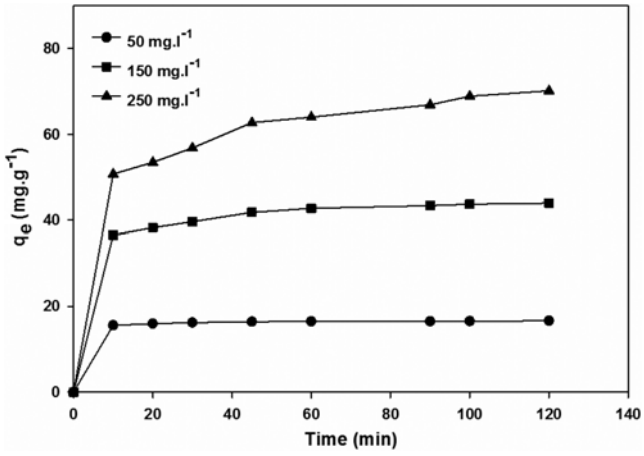

Fig. 6. Effect of initial concentration of Cr (VI) on removal efficiency (C_0=50, 150 and 250 mg·l^{-1}, T=45 °C, pH=2 and adsorbent dose=3 g·l^{-1}).

the negatively charged surface. The fact that the maximum adsorption of Cr (VI) occurred at acidic pH 2.0 may add some additional cost for the treatment of industrial wastewaters. However, such pH conditions may exist in some typical plant effluents such as electroplating.

2-2. Effect of Contact Time

The impact of contact time on the removal efficiency of Cr (VI) at two initial concentrations, 50 mg·l^{-1} and 150 mg·l^{-1}, pH of 2.0 and temperature of 25 °C, was studied and the results are depicted in Fig. 5. It is clear that about 90% of Cr (VI) removal occurred at the first 10 min and equilibrium was achieved after 120 min. At the beginning, the rate of Cr (VI) removal was high and then decreased gradually till it reached equilibrium. The transfer rate of Cr (VI) ions to the adsorbent surface is fast at the initial period of adsorption due to the availability of a plenty of active sites on the adsorption surface. However, at later times adsorption becomes slow as the result of the dominance of intraparticle diffusion mechanism for the diffusion of chromium into the adsorbent pores [31].

2-3. Effect of Initial Cr (VI) Concentration

The effect of initial metal concentration on the adsorption capacity was studied at several initial concentrations of Cr (VI) solutions in the range of 50-250 mg·l^{-1} at optimal pH 2.0 with 3 g·l^{-1} adsorbent at 45 °C and contact time of 120 min. Fig. 6 shows the equilibrium adsorption capacity of Cr (VI) increased from 16.61 mg·g^{-1} to 70.15 mg·g^{-1} when the Cr (VI) initial concentration increased from 50 to 250 mg·l^{-1}. Indeed, higher initial metal concentration provided a greater driving force for movement of chromium ions from aqueous phase to the solid surface .With increase of Cr (VI) ion concentration in the solution, interactions between Cr (VI) ions and the active sites on the activated carbon surface increased, which enhanced the adsorption process [32].

2-4. Effect of Temperature

To evaluate the effect of temperature, equilibrium experiments were conducted at different temperatures, 25, 35, 45 °C, at the initial concentration of 150 mg·l^{-1}, pH 2.0 and adsorbent dosage of 3 g·l^{-1}. The results are illustrated in Fig. 7. The Cr (VI) removal efficiency increased with an increase in temperature, indicating that the Cr (VI) adsorption is endothermic.

3. Adsorption Isotherm

To describe the adsorption equilibrium data of Cr (VI) ions onto

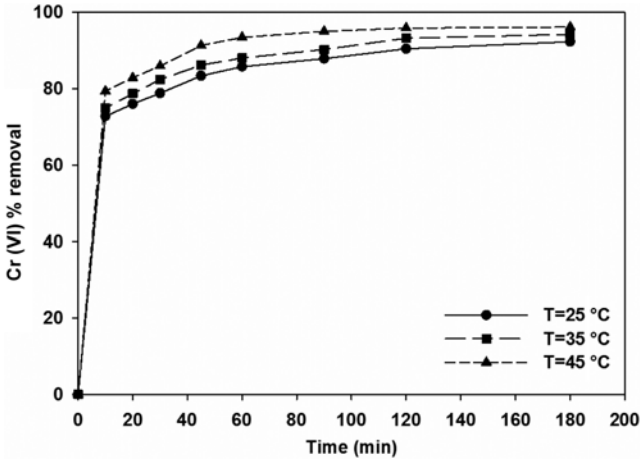

Fig. 7. Effect of temperature on removal efficiency of Cr (VI) (C_0= 150 mg·l^{-1}, pH=2 and adsorbent dose=3 g·l^{-1}).

the synthesized activated carbon, two isotherm models, Langmuir and Freundlich in nonlinear form, were used to fit the experimental data. The Langmuir adsorption isotherm assumes monolayer coverage of adsorbate on the adsorbent surface and a homogenous surface with equal active sites. The nonlinear form of the Langmuir isotherm is commonly described as [33]:

$$q_e = \frac{q_{max} b C_e}{1 + b C_e} \quad (4)$$

where q_e is the amount of the Cr (VI) ion adsorbed per unit mass of adsorbent at equilibrium (mg·g^{-1}), b is the Langmuir equilibrium parameter for adsorption (l·mg^{-1}), q_{max} denotes the maximum adsorption capacity (mg·g^{-1}) and C_e is the equilibrium adsorbate concentration (mg·l^{-1}).

The Freundlich isotherm model describes the adsorption equilibrium based on heterogeneous surface and indicates a multilayer adsorption on the adsorbent surface. The non-linearized form of the Freundlich equation is given as [33]:

$$q_e = k_F C_e^{1/n} \quad (5)$$

where k_F (mg·g^{-1}(l·mg^{-1})$^{1/n}$) and n are the constants indicative of adsorption capacity and intensity of the adsorption, respectively.

The parameters of the Langmuir and Freundlich isotherms were determined through nonlinear fit of experimental equilibrium data with model equations. The values obtained for the parameters of both isotherm models are listed in Table 4 along with regression correlation coefficients (R^2). The best fit was obtained with the Freundlich isotherm model by inspecting the correlation coefficient values (R^2>0.99), which indicated surface heterogeneity. Fig. 8 also shows the fitted curves by two isotherm models along with the experimental data for comparison.

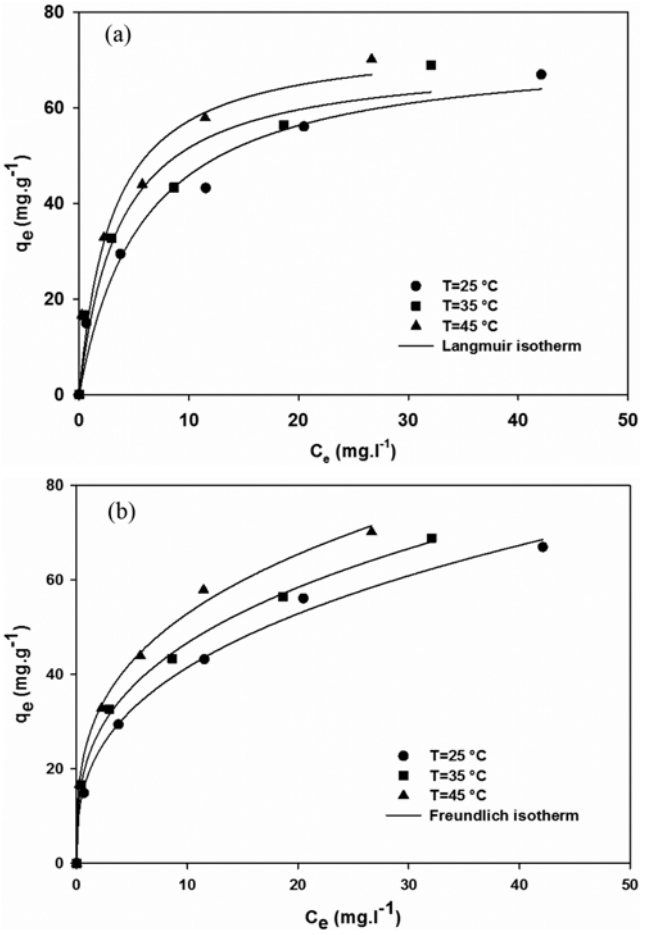

Fig. 8. Adsorption isotherm for adsorption of Cr (VI) onto the developed activated carbon fitted to the (a) Langmuir and (b) Freundlich isotherm models at different temperatures (pH= 2, adsorbent dose=3 g·l^{-1}).

4. Adsorption Kinetics

The study of adsorption kinetics provides useful information about the adsorption mechanism and rate-limiting step in the overall transport process. Different kinetic models have been used to interpret the adsorption data pertaining to heavy metal adsorption onto different adsorbents [34]. In the present work, to evaluate the kinetics of Cr (VI) adsorption onto the adsorbent, two models, the-pseudo-first-order and the pseudo-second-order kinetic models, were employed.

The pseudo-first-order equation is associated with physical adsorption in which weak interactions between the adsorbed metal ions and the adsorbent surface control the adsorption process [35]. The model is expressed as follows [36]:

Table 4. Constants of Langmuir and Freundlich isotherms for Cr (VI) adsorption onto the developed activated carbon

	Langmuir constant			Freundlich constant		
Temperature °C	b (l·mg^{-1})	q_{max} (mg·g^{-1})	R^2	k_F (mg·g^{-1}(l·mg^{-1})$^{1/n}$)	n	R^2
25	0.1705	72.83	0.9712	18.552	2.86	0.9963
35	0.2735	70.52	0.9482	22.1532	3.08	0.9988
45	0.3312	74.64	0.9538	26.0779	3.25	0.997

Table 5. Kinetic parameters of Cr (VI) adsorption onto the ADAS-based activated carbon

Initial concentration C_0 (mg/*l*)	Pseudo-first-order				Pseudo-second-order		
	$q_{e,exp}$ (mg·g^{-1})	k_1 (min^{-1})	$q_{e,cal}$ (mg·g^{-1})	R^2	k_2 (gmg^{-1}min^{-1})	$q_{e,cal}$ (mg·g^{-1})	R^2
50	16.61	0.0679	3.74	0.8835	0.0984	16.63	0.9999
100	32.84	0.0462	12.50	0.8937	0.0135	33.00	0.9992
150	43.95	0.0481	19.06	0.9222	0.0097	44.64	0.9993
200	57.91	0.0384	27.07	0.9008	0.0047	58.47	0.9979
250	70.15	0.0345	36.94	0.9139	0.0028	71.42	0.9964

$$\log(q_e - q_t) = \log q_e - \frac{k_1}{2.303}t \quad (6)$$

where q_e and q_t denote the amounts of Cr (VI) ions adsorbed (mg·g^{-1}) at equilibrium and at time t (min), respectively, and k_1 is the pseudo-first-order rate constant (min^{-1}).

The calculated values of q_e ($q_{e,cal}$) and k_1 were determined from the intercept and slope of the plot of $\log(q_e - q_t)$ versus t, respectively. In this work, time dependent adsorption data were used to fit the pseudo-first-order equation. These values along with regression correlation coefficients (R^2) are included in Table 5.

Kinetics of adsorption for some adsorbate-adsorbent systems may be better described by the pseudo-second-order equation. This kinetic model is based on the assumption that the adsorption is controlled by chemisorption [37]. The model is given as follows [36]:

$$\frac{t}{q_t} = \frac{1}{k_2 q_e^2} + \frac{1}{q_e}t \quad (7)$$

where k_2 is the rate constant of pseudo-second-order equation (g·mg^{-1}·min^{-1}). The values of k_2 and q_e are evaluated from the intercept and slope of plot t/q_t versus t, respectively. The rate constant k_2 and parameter q_e recovered through a linear fit of transient adsorption data with model equation as well as the regression coefficient (R^2) are listed in Table 5. It is clear that the values of adsorption capacities predicted by the pseudo-second-order kinetic were closer to the experimental values compared to those predicted by the pseudo-first-order kinetic model. Inspecting the fitting results in terms of regression correlation coefficient (R^2) also indicated a better performance of the pseudo-second-order kinetic model. Fig. 9(a) and (b) demonstrate the fitting results for the two used models.

5. Adsorption Thermodynamics

The investigation of adsorption thermodynamics gives an insight about heat management of the adsorption process to achieve efficient removal. Temperature-dependent experimental data obtained for the uptake of Cr (VI) onto the synthesized adsorbent were used to evaluate the thermodynamic parameters such as Gibbs free energy (ΔG^o), enthalpy (ΔH^o) and entropy (ΔS^o). The standard Gibbs free energy change (ΔG^o) is defined by the following equation:

$$\Delta G^o = -RT \ln K_{eq} \quad (8)$$

where T is the absolute temperature (K), R is the gas constant (8.314 J·mol^{-1}·K^{-1}) and K_{eq} is the equilibrium constant which relates concentration in adsorbed and bulk phase defined as follows:

$$K_{eq} = \frac{C_{ads}}{C_e} = \frac{C_0 - C_e}{C_e} \quad (9)$$

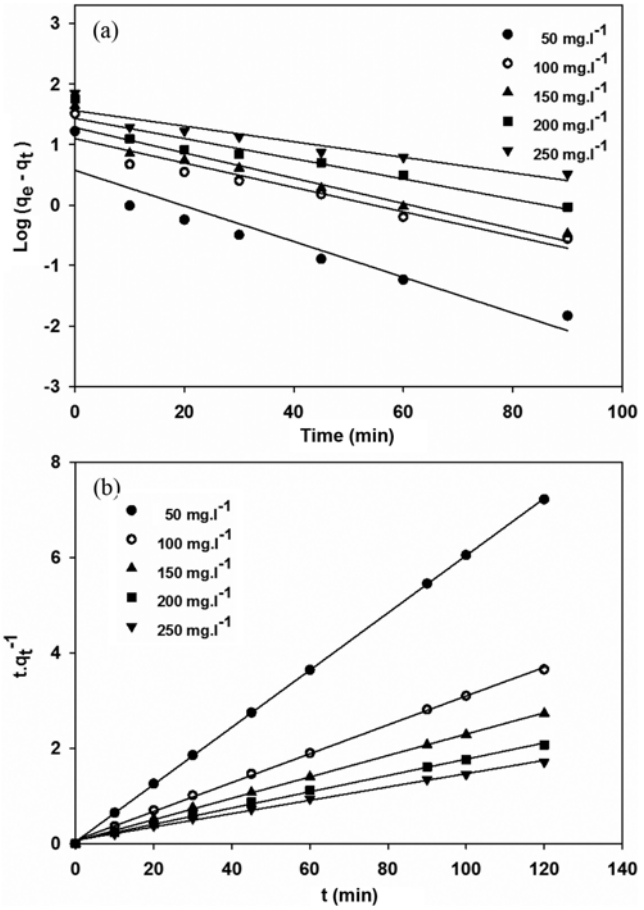

Fig. 9. (a) Pseudo-first-order and (b) Pseudo-second-order kinetics models of Cr (VI) adsorption on the ADAS-based activated carbon at different concentrations and temperatures (pH=2 and adsorbent dose=3 g·*l*$^{-1}$).

where C_{ads} and C_e indicate the amount of Cr (VI) concentration on the adsorbent and in the aqueous phase (mg·l^{-1}), respectively.

ΔH^o and ΔS^o which represent the change in enthalpy (kj·mol^{-1}) and entropy (kj·mol^{-1}·K^{-1}), respectively, are related with Gibbs free energy (ΔG^o) as follows:

$$\Delta G^o = \Delta H^o - T\Delta S^o \quad (10)$$

Substituting Eq. (8) into Eq. (10) gives:

$$\ln K_{eq} = -\frac{\Delta H^o}{RT} + \frac{\Delta S^o}{R} \quad (11)$$

Enthalpy (ΔH^o) and entropy (ΔS^o) changes were evaluated from

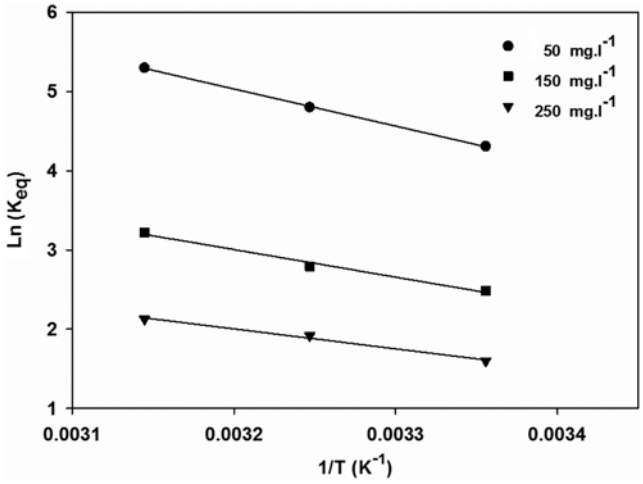

Fig. 10. Plot of ln K_{eq} vs. 1/T for Cr (VI) adsorption on the ADAS-based activated carbon.

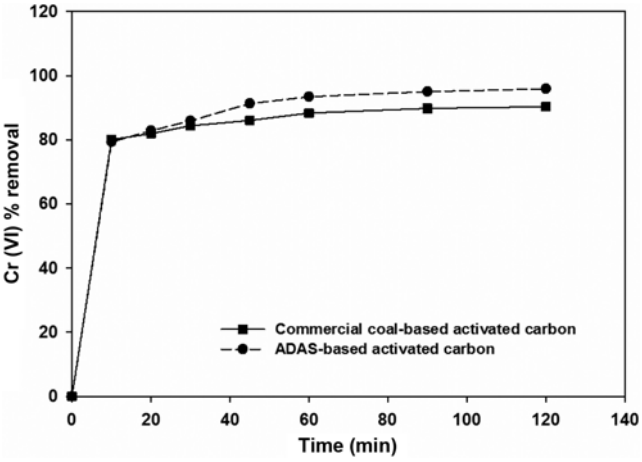

Fig. 11. Comparison of the ADAS-based activated carbon and commercial coal-based activated carbon for Cr (VI) removal (C_0=50 mg·l^{-1}, pH=2, T=45 °C and adsorbent dose=0.15 g·l^{-1}).

the slope and intercept of ln K_{eq} plot versus 1/T.

Fig. 10 depicts a linear plot of Eq. (11). The thermodynamic parameters recovered from the linear fitting of the temperature-dependent experimental data are summarized in Table 6.

The negative values of ΔG^o indicated the feasibility of the adsorption process and verified that the adsorption of hexavalent chromium on the prepared activated carbon occurred spontaneously. Following the values of ΔG^o in Table 6 reveals that spontaneity of the Cr (VI) adsorption onto the adsorbent increased with an increase in temperature and decreased with rise in initial Cr (VI) concentration. The decreasing trend of ΔG^o with an increase in temperature suggested that the adsorption was more favorable at higher temperature. The positive value of ΔH^o demonstrated the endothermic nature of the adsorption. This was supported by the increase in the Cr (VI) adsorption capacity of the adsorbent with an increase in temperature. The decreasing trend of ΔH^o values with increasing concentration may be due to the weak interactions between active sites on the adsorbent surface and adsorbed species at high surface coverage. The positive value of ΔS^o can be attributed to the increase in randomness and irregularity at the solid-solution interface during adsorption. Decreasing trend in ΔS^o values with an increase in concentration of Cr (VI) may be attributed to the decrease in randomness of adsorption at higher surface coverage. Indeed, at low concentration there are plenty of vacant active sites on the adsorbent surface which can be randomly occupied by the adsorbing species, while at higher concentration there are fewer active sites on the adsorbent surface; therefore, adsorbing species are enforced to bind with them more orderly. Some researchers [17,38] have reported similar results for the adsorption of Cr (VI).

6. Comparative Study

To assess the efficiency of the adsorption process for the removal of Cr (VI) by the developed ADAS-based activated carbon, a series of experiments were conducted with a kind of commercial coal-based activated carbon. The experiments were done at constant initial concentration of 50 mg·l^{-1}, solution pH 2.0, adsorbent dosage of 3 g·l^{-1} and temperature of 45 °C. Fig. 11 shows a comparison between the removal performance of the commercial activated carbon and the one synthesized in this work.

It is clear from Fig. 11 that the ADAS-based activated carbon demonstrated better performance compared to the commercial one for Cr (VI) removal from aqueous solution in spite of the similarity in pore size distribution. This can be attributed to the higher pore volume and specific surface area of the activated carbon produced in the present study.

7. Desorption Study

The reversibility of Cr (VI) ions adsorption onto the ADAS-based activated carbon was investigated by using different NaOH concentrations (0.1 to 0.5 N) as desorption agent. NaOH solution demonstrated good desorption efficiency. Desorption efficiency of Cr (VI) was enhanced with an increase in NaOH concentration. The best recovery was achieved with NaOH solution of 0.5 N. Adsorption-desorption efficiency of the prepared activated carbon after three cycles is presented in Table 7. The lower desorption efficiency in the first cycle can be assigned to the irreversible interactions between adsorbate and functional groups on the adsorbent surfaces, which becomes weaker due to successive contact with NaOH solution. After three cycles, desorption efficiency remained almost constant.

Table 6. Thermodynamic parameters for Cr (VI) ion adsorption onto the ADAS-based activated carbon at different temperatures

Initial Cr (VI) concentration (mg/*l*)	ΔH (kJ·mol^{-1})	ΔS (kJ·mol^{-1}K^{-1})	ΔG (kJ·mol^{-1})			R^2
			25 °C	35 °C	45 °C	
50	38.99165	0.166635	−10.665	−12.332	−13.998	0.9995
150	28.97129	0.117695	−6.1017	−7.2786	−8.4556	0.9877
250	20.91295	0.083575	−3.9923	−4.8281	−5.6638	0.99

Table 7. Adsorption and desorption efficiency of Cr (VI) ions after three cycles (50 mg·l^{-1}, pH 2.0 and 3.5 g·l^{-1} of the adsorbent)

Cycle	1	2	3
% Adsorption	94	74	69.2
% Desorption	61.84	72.87	78.7

Therefore, the results of adsorption-desorption experiments confirmed that this adsorbent can be frequently used for the removal of Cr (VI) from water and wastewater.

CONCLUSIONS

A new activated carbon was developed from aerobically digested activated sludge (ADAS) as a low cost suitable precursor with good physiochemical characteristics and was efficiently used for the removal of chromium (VI) ion from wastewater. Mesoporous activated carbon was produced with high surface area of 760 m^2/g and total pore volume of 0.8383 cm^3/g. The adsorption properties of the developed activated carbon were examined via a series of experimental runs conducted at different conditions. The results revealed that the solution pH, initial metal concentration, dosages of adsorbent, contact time and temperature significantly influenced the Cr (VI) removal efficiency. Maximum Cr (VI) adsorption was found to be 70.15 mg·g^{-1} at pH 2.0, initial concentration of 250 mg·l^{-1}, adsorbent dosage of 3 g·l^{-1}, contact time of 120 min and temperature of 45 °C. The equilibrium, kinetics and thermodynamic analyses were carried out to interpret the adsorption capacity, adsorption mechanism and thermal nature of Cr (VI) adsorption on the new adsorbent. The calculated thermodynamic parameters indicated the spontaneous and endothermic nature of Cr (VI) adsorption on the adsorbent developed in the present work. This study clearly demonstrates the superior performance of the ADAS-based activated carbon compared to the commercial coal-based activated carbon. The results achieved in the present work are promising because a dual benefit can be taken using activated sludge as a precursor to make an efficient adsorbent for Cr (VI) removal from wastewater. On one hand, using such low cost material would improve the adsorption process economy. And on the other, using activated sludges for this purpose could help to diminish the environmental harms due to their dumping in nature.

REFERENCES

1. A. A. Attia, S. A. Khedr and S. A. Elkholy, *Braz. J. Chem. Eng.*, **27**, 183 (2012).
2. N. R. Bishnoi, M. Bajaj, N. Sharma and A. Gupta, *Bioresour. Technol.*, **91**, 305 (2004).
3. V. K. Gupta, A. Rastogi and A. Nayak, *J. Colloid Interface Sci.*, **342**, 135 (2010).
4. K. Muthukumaran and S. Beulah, *Procedia Environ. Sci.*, **4**, 266 (2011).
5. S. A. Cavaco, S. Fernandes, M. M. Quina and L. M. Ferreira, *J. Hazard. Mater.*, **144**, 634 (2007).
6. P. Lakshmipathiraj, G. Bhaskar Raju, M. Raviatul Basariya, S. Parvathy and S. Prabhakar, *Sep. Purif. Technol.*, **60**, 96 (2008).
7. P. Venkateswaran and K. Palanivelu, *Sep. Purif. Technol.*, **40**, 279 (2004).
8. V. Song, C. Williams and R. Edyvean, *Desalination*, **164**, 249 (2004).
9. M. Bansal, D. Singh and V. K. Garg, *J. Hazard. Mater.*, **171**, 83 (2009).
10. A. Hafez, M. El-Manharawy and M. Khedr, *Desalination*, **144**, 237 (2002).
11. S. S. Baral, S. N. Das and P. Rath, *Biochem. Eng. J.*, **31**, 216 (2006).
12. L. Levankumar, V. Muthukumaran and M. B. Gobinath, *J. Hazard. Mater.*, **161**, 709 (2009).
13. R. Shankar Singh and M. Kumar Mondal, *Korean J. Chem. Eng.*, **29**, 1782 (2012).
14. M. A. A. Zaini, Y. Amano and M. Machida, *J. Hazard. Mater.*, **180**, 552 (2010).
15. K. K. Krishnani, X. Meng, C. Christodoulatos and V. M. Boddu, *J. Hazard. Mater.*, **153**, 1222 (2008).
16. S. Babel and T. A. Kurniawan, *Chemosphere.*, **54**, 951 (2004).
17. A. K. Giri, R. Patel and S. Mandal, *Chem. Eng. J.*, **185**, 71 (2012).
18. Z. A. Al-Othman, R. Ali and M. Naushad, *Chem. Eng. J.*, **184**, 238 (2012).
19. M. Kobya, *Bioresour. Technol.*, **91**, 317 (2004).
20. V. Malkoc, Y. Nuhoglu and M. Dundar. *J. Hazard. Mater.*, **138**, 142 (2006).
21. T. Karthikeyan, V. Rajgopal and L. R. Miranda, *J. Hazard. Mater.*, **124**, 192 (2005).
22. K. Selvaraj, S. Manonmani and S. Pattabhi, *Bioresour. Technol.*, **89**, 207 (2003).
23. C. Liu, Z. Tang, Y. Chen, S. Su and W. Jiang, *Bioresour. Technol.*, **101**, 1097 (2010).
24. N. R. Khalili, M. Campbell, G. Sandi and V. Gola, *Carbon*, **38**, 1905 (2000).
25. L. S. Clesceri, A. E. Greenberg and R. R. Trussell, *Standard methods for examination of water and wastewater 17th Ed.* (1989).
26. K. S. W. Sing, D. H. Everett, R. A. W. Haul, L. Moscou, R. A. Pierotti, J. Rouquerol and T. Siemieniewska, *Pure Appl. Chem.*, **57**, 603 (1985).
27. V. Vinodhini and N. Das, *Am-Euras. J. Sci. Res.*, **4**, 324 (2009).
28. J. L. Gardea-Torresdey, K. J. Tiemann, V. Armendariz, L. Bess-Oberto, R. R. Chianelli, J. Rios, J. G. Parsons and G. Gamez, *J. Hazard. Mater.*, **80**, 175 (2000).
29. S. Basha, Z. V. P. Murthy and B. Jha, *Chem. Eng. J.,* **137**, 480 (2008).
30. H. S. Deveci and Y. Kar, *J. Ind. Eng. Chem.*, **19**, 190 (2012).
31. R. Kumar, N. R. Bishnoi and K. Bishnoi, *Chem. Eng. J.*, **135**, 202 (2008).
32. F. Ghorbani, H. Younesi, S. Ghasempouri, A. Zinatizadeh, M. Amini and A. Daneshi, *Chem. Eng. J.*, **145**, 267 (2008).
33. G. Limousin, J. P. Gaudet, L. Charlet, S. Szenknect, V. Barthes and M. Krimissa, *Appl. Geochem.*, **22**, 249 (2007).
34. K. Wong, C. Lee, K. Low and M. Haron, *Chemosphere.*, **50**, 23 (2003).
35. H. Radnia, A. A. Ghoreyshi, H. Younesi and G. D. Najafpour, *Desalin. Water Treat.*, **50**, 348 (2012).
36. Y. Ho and G. McKay. *Process Biochem.*, **34**, 451 (1999).
37. K. Low, C. Lee and S. Liew, *Process Biochem.*, **36**, 59 (2000).
38. E. Oguz, *Colloids Surf., A.*, **252**, 121 (2005).